

The effect of temperature and wetting–drying cycles on soil wettability: Dynamic molecular restructuring processes at the solid–water–air interface

Joerg Bachmann  | Steffen Söffker | Nasrollah Sepehrnia  |
Marc-O. Goebel | Susanne K. Woche

Institute of Soil Science, Leibniz
Universität Hannover, Hannover,
Germany

Correspondence

Joerg Bachmann, Institute of Soil Science,
Leibniz Universität Hannover,
Herrenhäuser Str. 2, 30419 Hannover,
Germany.
Email: bachmann@ifbk.uni-hannover.de

Funding information

Research Foundation

Abstract

The impact of heat treatment and wetting–drying cycles on the wetting properties of sandy forest soils was explored. Topsoil and upper subsoil were sampled at three beech forest sites in northern Germany. The air-dried soils were treated at 20, 40 and 80°C for 24 h, with materials treated at 20°C serving as reference. After wetting, materials were air-dried or shock-frozen in liquid N₂ and freeze-dried. Interfacial properties were monitored by sessile drop contact angles (CAs) and X-ray photoelectron spectroscopy (XPS), which provide physical and chemical information on the outermost particle interface layer. CAs of reference samples were around 90° and significantly increased after 80°C-treatment to >90°, whereas 40°C-treatment had in comparison to reference soils no distinct impact on CA. Depending on the initial temperature treatment, air-drying after wetting decreased CA to 60–80% and shock-freezing and freeze-drying decreased CA to 10–50% of the reference value. Results suggest that shock-freezing may preserve the organic matter molecular structure that prevails during contact with water at the solid–liquid interface, thus indicating the wettability of the wet surface. Generally, wetting–drying cycles had the least impact on 80°C-treated material. XPS analysis confirmed dynamic interfacial molecular restructuring processes by changes in O and C content and the content of non-polar C compounds. A second heat treatment after two wetting–drying cycles again proved the distinct and pronounced impact of 80°C-treatment on CA, especially with prior shock-freezing and freeze-drying. In conclusion, the findings of our study indicate a sensitive and partly reversible reorganization of the solid interfacial wetting properties. Results may conceptually be used to develop dynamic wettability models, which are needed to simulate the sensitive interplay between wettability and dynamic soil hydraulic functions at sites that are exposed to intensive and periodic moisture fluctuations.

This is an open access article under the terms of the Creative Commons Attribution-NonCommercial-NoDerivs License, which permits use and distribution in any medium, provided the original work is properly cited, the use is non-commercial and no modifications or adaptations are made.

© 2021 The Authors. *European Journal of Soil Science* published by John Wiley & Sons Ltd on behalf of British Society of Soil Science.

Highlights

- $T > 40^{\circ}\text{C}$ increased contact angle; after wetting contact angle depended on how the water was removed
- Shock-freezing and freeze-drying preserves contact angle of the wetted state
- Contact angle changes confirm interface molecular restructuring due to heat treatment or wetting
- Contact angle change goes along with changes in element content within XPS analysis depth

KEYWORDS

Contact angle, Heat treatment, Interfacial chemical composition, Sandy forest soil, Wetting-drying cycles, X-ray photoelectron spectroscopy (XPS)

1 | INTRODUCTION

Soil as a porous three-phase system is characterized by a tremendously high surface area to volume ratio of the solid phase. The majority of processes in soils are in the stricter sense “interfacial processes” because they normally proceed at soil particle surfaces, a fact that is not always realised. Up to now, the common practice is to evaluate soil bulk parameters for the analysis of soil processes and soil ecosystem services. However, to understand soil-specific processes thoroughly, a stronger focus on particle interfacial properties should be taken into account. Soil water repellency (SWR), for example, is considered a significant interface phenomenon that impacts soil functioning as particle wettability affects physical (e.g., water distribution and dynamics), chemical (e.g., solute transport processes) and biological (e.g., microbial abundance) properties.

It has been known for decades that SWR is observed within a widerange of climatic conditions, where it is associated with many different soil and vegetation types and land-use systems (e.g., DeBano, 2000; Doerr, Shakesby, & Walsh, 2000; Ellies & Hartge, 1994; Jaramillo, Dekker, Ritsema, & Hendrickx, 2000; Moore & Blackwell, 2001; Scott, 2000; Woche et al., 2005). Clean mineral surfaces (free of organic matter) are mostly hydrophilic because they are usually electrically charged or expose polar functional groups, both of which support the wetting process at the three-phase boundary (Lewin, Mey-Marom, & Frank, 2005; Tschapek, 1984). Regarding the soil mineral phase, the surface charge originates mainly from clay minerals and Fe/Al-(hydr)oxides, which both determine the physicochemical behaviour of the soil (Sposito, 1989; Stevenson, 1994), including important processes such as flocculation or dispersion of colloidal particles (e.g., Dultz, Steinke, Mikutta, Woche, & Guggenberger, 2018). In this respect, coatings consisting

of so-called low-energy organic components are often water repellent and very effective in masking hydrophilic surface properties of minerals. Such an organic layer, in extreme cases only a monolayer, may render glass or mineral surfaces hydrophobic (Bos, van der Mei, & Busscher, 1999; Lewin et al., 2005; Šolc, Tunega, Gerzabek, Woche, & Bachmann, 2015; Tschapek, 1984; Zisman, 1964). Amphiphilic components can increase water repellency upon drying when non-polar functional groups are assumed to be oriented towards pore spaces (Doerr et al., 2000). The predicted higher frequency of extended droughts due to climate change in many regions worldwide suggests the occurrence of seasonal SWR to become more frequent in the future, with negative implications for soil functioning (Goebel, Bachmann, Reichstein, Janssens, & Guggenberger, 2011). A high level of actual SWR has a strong impact on soil hydrology, infiltration, erosion and plant growth. Using model experiments with alfalfa (*Medicago sativa*), Hassan, Woche, and Bachmann (2014) found that increasing levels of SWR significantly decreased plant growth, demonstrating the importance of soil wettability for complex plant-soil interactions.

Soil particle interfaces normally are formed by an extremely heterogeneous arrangement of organic and inorganic components (Kögel-Knabner et al., 2008), which together build up the reactive biogeochemical interface (Totsche et al., 2010). There is increasing evidence that there also exists a zonal gradient of the chemical composition of soil organic matter (SOM) attached to mineral surfaces (Kleber, Sollins, & Sutton, 2007). Hence, analysing the average chemical composition of the bulk soil may not reflect the relevant properties of the thin reactive interface, which is commonly less than 1% of the soil dry mass by weight, but may control the process of interest. Regarding the soil organic compounds, there is a debate on what type of organic matter is attached more

closely to the mineral and which components are oriented towards the liquid phase (e.g., Kleber et al., 2007). Beside the chemical specification, which is already intensively discussed in the literature (e.g., Mikutta et al., 2009), the definition of effective and physically sound parameters to better describe relevant hydraulic, mechanical or physico-chemical soil properties is still pending. In this context, another important aspect is the dynamics of wetting properties with time. The stability of SWR, often termed as persistency, is commonly assessed by the water drop penetration time test (WDPTT; Doerr et al., 2000). However, previous studies show that this test is inappropriate for many soils with intermediate (“subcritical”) stages of SWR due to its insensitivity to material characterized by contact angles (CA) $< 90^\circ$ (e.g., Bachmann, Deurer, & Arye, 2007). Regarding the wetting properties of many soils, in particular this subcritical range is important, especially for the estimation of in situ water storage capacity (Deurer & Bachmann, 2007; Täumer, Stoffregen, & Wessolek, 2005), as well as for the interpretation of field observations such as the temporal development of surface runoff and infiltrability (Beatty & Smith, 2013; Clothier, Vogeler, & Magesan, 2000).

From the above observations it is evident that systematic investigations on natural soil materials comprising a wide range of SWR stages are needed to study time-dependent wettability effects. Preliminary research shows that soil wettability can be modified by moderate heat treatment without changing other significant factors such as carbon content, texture and pH (Dekker, Ritsema, Oostindie, & Boersma, 1998; Diehl et al., 2014; Gaj et al., 2019; Reszkowska, Bachmann, Lamparter, Diamantopoulos, & Durner, 2014). The strategy of the present study was therefore to expose air-dry water-repellent sandy soils to different temperatures (20°C, 40°C and 80°C) and to compare their interfacial properties after subsequent repeated wetting–drying cycles, simulating corresponding cycles in the field. Sample drying after wetting was achieved either by air-drying (slow drying, evaporation from the liquid state) or by shock-freezing in liquid N₂ and subsequent freeze-drying (evaporation from the frozen state). The latter method was intended to “freeze” the interfacial properties prevailing during contact with water and thus to minimize surface modifications that may occur during drying in contact with air, similar to in situ evaporation. To test the extent of reversibility of the acquired wettability state, in a final step, the drying procedure was reversed; that is, the formerly air-dried samples were shock-frozen and freeze-dried and vice versa. Finally, to test the persistency of the wetting properties observed after several wetting–drying cycles, materials were exposed to a second heat treatment. To summarize, the major objective of the present study with

its complex experimental design is to prove the capability of selected parameters to capture quantitatively the dynamically changing wettability of soil particles in contact with either water or air. The detailed objectives of the present study are: (a) to characterize the wetting properties for each treatment by sessile drop CA, (b) to apply X-ray photoelectron spectroscopy (XPS) for selected samples to characterize the interface chemical composition as affected by heat treatment and wetting–drying cycles, and (c) to combine CA and XPS data to directly prove the relationship between interface chemical composition and wetting properties under different environmental conditions.

1.1 | Theoretical framework and suitable analytical techniques

1.1.1 | Structure, evaluation and modification of soil particle interfaces

The complex structure of organic coatings on soil particles as a multicomponent interface is not precisely defined (e.g., Schaumann, LeBoef, DeLapp, & Hurraß, 2005). In order to quantify conformational changes of interface functional groups, Ferguson and Whitesides (1992) analysed polyethylene with defined surface modifications with several interface-sensitive techniques (CA measurement, XPS, and attenuated total reflectance Fourier-transform infrared spectroscopy [ATR-FTIR]). These techniques probe different depths of the material and, consequently, Ferguson and Whitesides (1992) defined specific “interphases” according to the physical depth probed by the respective techniques (Figure 1). The “CA interphase” refers to the outer 0.5–1.0 nm layer, which has chemical compounds that determine the wetting properties. Next, the “XPS interphase” refers to approximately the outer 1–3 nm, the analysis depth of XPS. Additionally, the “ATR-FTIR interphase”, the deepest interphase of interest, refers to the outer 1 µm or deeper. As shown by the present study, the information provided by CA and XPS gives information on the relationship between chemical composition, its changes with applied treatment, and the measured CA for water drops.

Ferguson and Whitesides (1992) reported further that in some cases functional groups exist outside the CA interphase, located too deep to influence wetting. They are nonetheless accessible to reagents in solution and Ferguson and Whitesides (1992) termed the portion of the solid where this type of interaction is possible the “sub-CA interphase”. The depth of the sub-CA interphase is between that of the XPS and the ATR-FTIR interphases. It is determined by permeability, pore structure and liquid–solid interactions and is generally less well

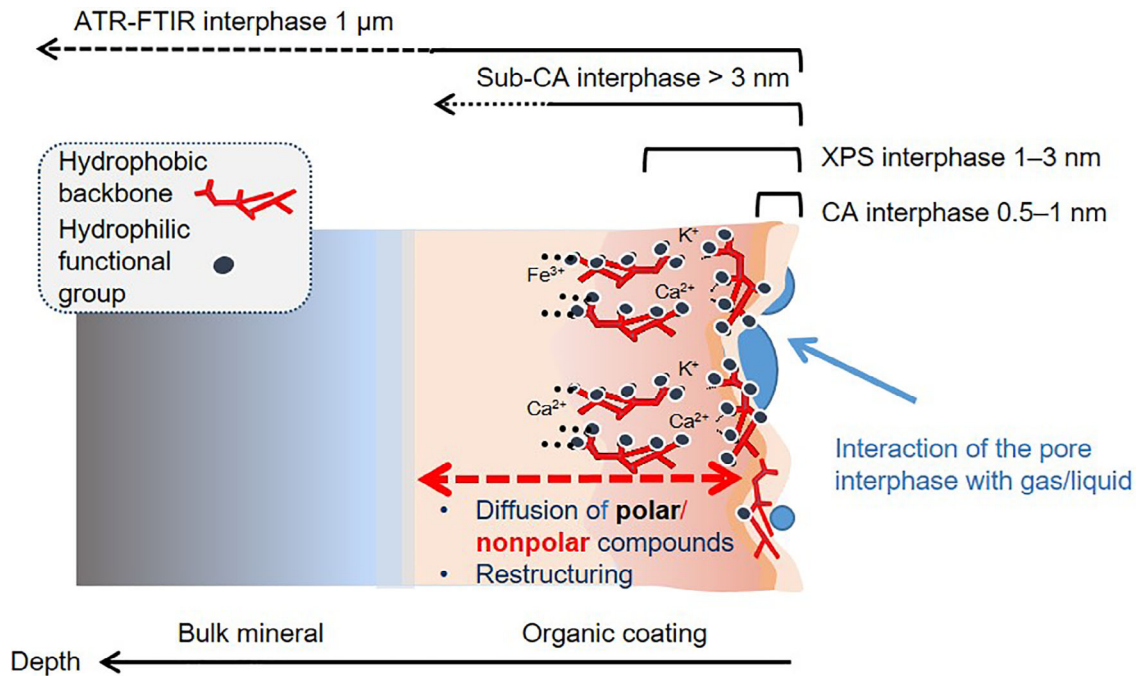


FIGURE 1 Schematic representation of the different analytical penetration depths at the solid interphase. Figure redrawn after Ferguson and Whitesides (1992) and Ellerbrock, Gerke, Bachmann, and Goebel (2005). ATR-FTIR, attenuated total reflectance Fourier-transform infrared spectroscopy; CA, contact angle; XPS, X-ray photoelectron spectroscopy

defined than the depth associated with the analytical techniques. Structural reorganization processes may modify the chemical composition within the XPS analysis depth. In the case of OM-coated soil particles, this may result in varying amounts of the underlying mineral within the analysis depth. At present, corresponding and systematic studies for soil particles are rare, as outlined below.

By investigating the relationship between moisture content and wettability, Chassin, Jounay, and Quiquampoix (1986) reported changes in surface free energy of Ca-montmorillonite as a function of water content. They found that the main contribution to the surface free energy came from dispersion forces, originating from surface oxygen atoms of the SiO_4 tetrahedra, whereas polar forces are derived from exchangeable cations. The adsorption of water molecules was found to substantially modify the surface free energy of the clay. Applying a modified sessile drop method by using pressed clay samples, Chassin et al. (1986) found that the surface free energy of the clay decreased continuously from 180 mJ m^{-2} , which corresponds to a zero CA wetting regime, to the value of water (72 mJ m^{-2}) when the water content of the clay exceeds 50% (by mass). In principle, these results imply that the silicate surface itself no longer influences the surface properties of the moist surface. This insight fits well with the observation that drying of soils due to seasonal variation in precipitation and

evapotranspiration periodically modifies SWR due to a masking effect through adsorbed water films or water bodies (Bachmann et al., 2007; Buczko, Bens, & Hüttel, 2005; Keizer et al., 2008; Leighton-Boyce et al., 2005). At this point it should be stated that the results derived from measurements of soil particles do not indicate if the decreasing surface free energy is specifically caused by the increasing amount of water bodies just forming composite surfaces according to the Cassie-Baxter model (Good, 1992). Alternatively, in addition, changes in the molecular configuration of the solid interface itself might also be responsible for the observed decrease in surface free energy, a hypothesis that has not yet been proved experimentally for soil particles.

1.1.2 | Specific contribution of X-ray photoelectron spectroscopy

XPS is capable of analysing chemical composition and the chemical state of elements with an analysis depth of only ca. 0.5 nm to a maximum depth of 10 nm (Ahmad et al., 2017). Although XPS is frequently used in material sciences and nanotechnology, it has only been scarcely applied in environmental and soil science (e.g., Abe & Watanabe, 2004; Flogéac et al., 2005; Gerin, Genet, Herbillon, & Delvaux, 2003; Mikutta et al., 2009; Woche et al., 2017). Dang-Vu et al. (2009) used XPS to study

particle wettability and surface composition of oil sands. They found a correlation between solid wettability and the Si, Al, C and S content with more hydrophilic solids for the lowest C and S and highest Si and Al contents. Kobayashi and Matsui (2003) used XPS to explain the relationship between water repellency and chemical composition of organic matter in hydrophobic forest soils. XPS revealed that water repellency was related to components of low binding energy, corresponding to C–C, C–H and C=C bonds (representing aliphatic organic matter components). Woche et al. (2017) found for natural soil materials from a soil chronosequence that the C content was positively correlated with CA. The contents of O and mineral-derived cations were negatively correlated with CA, suggesting an increasing organic coating of the minerals that progressively masked the underlying mineral phase with increasing soil age. The atomic O/C ratio was found to be closely negatively correlated with CA, which applied as well to further sample sets of different texture and origin. Woche et al. (2017) concluded that the surface O/C ratio is a general chemical parameter linking surface wettability and surface element composition. With the findings so far as a conceptual base, we will use the O/C ratio as an already derived chemical proxy and the amount of non-polar C compounds (Woche et al., 2017) to explain observed wetting properties independent of tested soil, wetting history, and heat treatment.

1.1.3 | Soil particle interface characterization by contact angle measurements

A solid–liquid CA is the angle formed at the three-phase contact of a drop of liquid with a surface and often termed as the apparent CA. Due to energy barriers caused by roughness, chemical heterogeneity or air inclusion, the apparent CA is not necessarily the equilibrium and thermodynamically sound CA, reflecting the lowest surface free energy of the system (Adamson, 1990). The apparent (visible) CA may be observed after liquid has been added to a surface; the observed CA lies between the equilibrium CA and the advancing CA, which appears during active advancement of a wetting front, for example after adding liquid to the sessile drop. Removal of drop of liquid leads to a receding CA, which is smaller than the advancing or equilibrium CA (Ferguson & Whitesides, 1992). A schematic representation of various methods adapted to soil particles and the governing equations to calculate the CA can be found in Bachmann, Woche, Goebel, Kirkham, and Horton (2003). Ideal surfaces for surface analysis are considered as smooth, homogeneous, chemically inert and mechanically rigid. On ideal

planar surfaces, two approaches to determine the equilibrium CA, θ_e , exist: force balance and minimum surface free energy. In Equation (1), the subscripts *S*, *L* and *V* represent the interfacial tensions of the solid, liquid and vapour phases. They are often regarded as forces per unit length (N m^{-1}) and a horizontal force balance at the contact line is imposed: $\gamma_{SL} + \gamma_{LV} \cos\theta_e = \gamma_{SV}$. Often ignored is the force component needed to accomplish the equilibrium of force components in the plane of the surface as given in Equation (1). This force is acting normally on the solid surface and originates from the strain field in the solid under the drop (for further explanation, see Good, 1992). In the energy-based concept, the interfacial tensions are regarded as energies per unit area (J m^{-2}) and the energy change due to a small displacement of the liquid–vapour interface is assumed to vanish in the CA equilibrium state. Either approach gives rise to the Young equation (Equation (1)), which has been qualitatively described by Young (1805):

$$\cos\theta_e = (\gamma_{SV} - \gamma_{SL}) / \gamma_{LV}. \quad (1)$$

The energy view provides a simple approach to surfaces that are patterned or rough, irrespective of whether the patterning is chemical or topographic (Bachmann & McHale, 2009). The quantity $\cos\theta_e$ is proportional to the difference between γ_{SV} and γ_{SL} , which is related to the type of functional groups at the solid interface (Zisman, 1964). It is notable that when $\gamma_{SV} - \gamma_{SL} > \gamma_{LV}$ then $\cos\theta_e$ equals one, that is $\theta_e = 0^\circ$, indicating complete wettability (Padday, 1992). $\theta_e > 0^\circ$ and $< 90^\circ$ indicates reduced wettability (subcritical repellency) and $\theta_e \geq 90^\circ$ indicates extreme water repellency or hydrophobicity.

The above concepts of surface physicochemistry allow a straightforward characterization of solid surfaces, including surface free energy components and respective hydrophobicity/hydrophilicity status (Chibowski, Holysz, & Szces, 2017; Drehlich et al., 2019; Good, 1992; van Oss, Chaudhury, & Good, 1988; van Oss & Giese, 1995). Contact angle measurement is limited for powdered samples or porous media such as packed soil due to several factors. Here, surface characterization has principally to deal with non-ideal conditions, as soil particle surfaces are typically rough, chemically extremely heterogeneous and reactive. Especially contact with water or soil solution may impose effects through sorption, swelling or dissolution processes (Diehl et al., 2014; Shchegolikhina et al., 2014). Therefore, some preliminary remarks regarding the evaluation of soil particle surface wetting properties seem appropriate (e.g., Drehlich et al., 2019).

Attempts to improve sample properties before measurement, for example smoothing through pressing particles to pellets to reduce surface roughness and porosity,

may reduce the macroscopic physical sample roughness, but are expected to modify the particle interfacial properties to some extent while these properties might be the focus of interest. Hence, the determination of soil particle interfacial properties is challenging and consistency of applied methods has to be evaluated according to the objective of the respective study. In the present paper we will focus on the application of the sessile drop method (SDM; Good, 1992). In the case of soil particles, the SDM has the advantage of a high spatial resolution (mm scale), for example when applied to undisturbed larger soil sample surfaces (Bachmann, Goebel, & Woche, 2013; Krueger et al., 2018; Lamparter, Bachmann, & Woche, 2010; Moradi et al., 2012;). The SDM needs only a low amount of sample material (< 1 g) for CA determination of disturbed material with a reasonable number of replicates. As only a low amount of testing liquid is required (drop volume 1 μL), soil solution might also be considered for CA evaluation. A further advantage compared to other methods is that the SDM is not restricted to $\text{CA} < 90^\circ$. Other commonly used methods that are based on the penetration of a liquid into a packing of particles may have further unexpected effects on CA measurement due to additional impact factors such as wetting time, pore size and inertial effects, or dynamic CA affected by the liquid penetration velocity inside the pores may significantly affect the results (Lavi, Marmur, & Bachmann, 2008). Even more importantly, it is not necessary to evaluate pore shape factors using a reference liquid (Chibowski et al., 2017; Siebold, Walliser, Nardin, Oppliger, & Schultz, 1997) that may interact with reactive or soluble components of the soil matrix. In principle, all the experimental methods for the determination of particle wettability have some doubts and the obtained results may be debatable (Chibowski et al., 2017), especially for heterogeneous soil particles. Nevertheless, there are several studies that successfully applied the SDM on soil particles (e.g., Bachmann et al., 2020; Gaj et al., 2019; Krueger, Boettcher, Schmunk, & Bachmann, 2016; Woche et al., 2017). A comprehensive theoretical approach for solid surface characterization based on sessile drop CA measurements on self-supported particle layers of clay mineral surfaces was proposed by van Oss, Giese, and Constanzo (1990), who aimed to define the wettability status of clay mineral particles suspended in water. The authors found that the transition between hydrophobicity and hydrophilicity is not generally at a CA around 0° but can reach a CA of about 50° , indicating again the importance of CA measurements in the range between 0 and 90° for soil or mineral particles.

A study on the simultaneous effects of chemical heterogeneity and roughness on partly wetted surfaces has been conducted by Bachmann and McHale (2009). In

their model for idealized spherical particles, roughness first transforms the Young's law-CA to the Wenzel-CA (Adamson, 1990), followed by the bridging effect, transforming the Wenzel-CA via a Cassie-Baxter equation (Adamson, 1990) to a combined Wenzel Cassie-Baxter wetting regime (Bachmann & McHale, 2009). The outcomes of the developed analytical model were compared with numerical simulations to predict roughness and heterogeneity effects for an array of spherical particles with a known intrinsic CA, which was measured on ideal smooth surfaces. Model calculations based on the Lattice-Boltzmann simulation technique showed a good agreement between pore-scale simulations of a CA (Kang, Lourenco, & Yan, 2018) and the analytical approach proposed by Bachmann and McHale (2009) for $\text{CA} > 30^\circ$, showing the general potential of the SDM to detect changes in wettability for powders with wetting properties ranging from intermediate water repellency to hydrophobicity (Kang et al., 2018; Saulick, Lourenco, Baudet, Woche, & Bachmann, 2018). In summary, sessile drop CA determination on rough particles suggests a plausible relationship between measured (apparent) CA and chemical properties of the solid interface. To reduce the sources of uncertainty, in the present study, we will compare surfaces of similar topography, but with different levels of water repellency.

2 | MATERIALS AND METHODS

2.1 | Soil material

Topsoil and upper subsoil material was sampled at three beech (*Fagus sylvatica*) forest sites (Sellhorn, S, Unterlüß, U, and Calvörde, C) along a NW–SE precipitation gradient in northern Germany (Figure S1, Supporting Information) with similar mean annual temperatures between 8.5 and 9.1°C . The sites are not affected by groundwater (groundwater level below 3 m depth). Soil was collected from a sampling area of about 2 m^2 from approximately 0–2 cm (topsoil) and 4–10 cm depth (subsoil). All sites were similar in texture and pH. The material was air-dried, sieved $<2\text{ mm}$, and stored in plastic bags at room temperature until further treatment about 7 months later. To prove a possible impact of the plastic material on the contact angle, we stored wettable silt material in a glass container and in a plastic bag (about 2 g in a 4-L plastic bag), for about 4 weeks. The material in the plastic bag was repeatedly brought into intensive contact with the plastic by mechanically kneading the bag. The contact angle of both samples was identical (glass bottle, 14.4° SD 4.4° ; plastic bag, 12.2° SD 5.2°). It was evident that alteration

due to contact with plastic would be negligible because the soil/plastic mass ratio in the case of our samples was considerably larger. Basic soil physical and chemical properties can be found in Table 1.

2.2 | Sample preparation

Figure 2 shows a scheme of the treatments. Air-dry topsoil (index 't') and subsoil (index 's') samples were exposed to heat treatment for 24 h in a climate-controlled chamber (20°C) and a drying oven (40, 80°C), respectively. Sample material was split into two portions, transferred to polyethylene (PE) containers and wetted by adding ultrapure water under gentle stirring with a glass rod. The mass of added water was equivalent to the gravimetric water content in equilibrium with a matric potential of about -1 to -2 hPa (determined independently in disturbed columns).

Due to the similar texture (Table 1), the same amount of water was added to all materials. After moistening, the PE containers were closed and the wetted material was left for 3 days, interrupted once a day for gentle stirring with a glass rod for a few seconds. After this wetting phase the material was either air-dried at room temperature in a climate-controlled chamber (variant 'A') or shock-frozen and freeze-dried (variant 'N') during a period of 4 days. For shock-freezing, the closed PE container was dipped in liquid N₂ for 10 s and the contents subsequently freeze-dried. This wetting-drying cycle was

repeated once (variants 'A_A' and 'N_N', respectively). In a final step, the samples were split again into two sets. One set was wetted again in the same way; however, the drying procedure was reversed, that is, the initially air-dried samples were shock-frozen and freeze-dried and the initially shock-frozen and freeze-dried samples were air-dried (variants 'A_A_N' and 'N_N_A', respectively). In total, each sample was wetted and dried three times. The other complete sample set underwent a second heat treatment at 20°C, 40°C, and 80°C, but now after two wetting-drying cycles with either air-drying (A_A) or shock-freezing and freeze-drying (N_N), respectively. These samples were wetted and dried two times. All treatments resulted in a total of 199 samples (Figure 2).

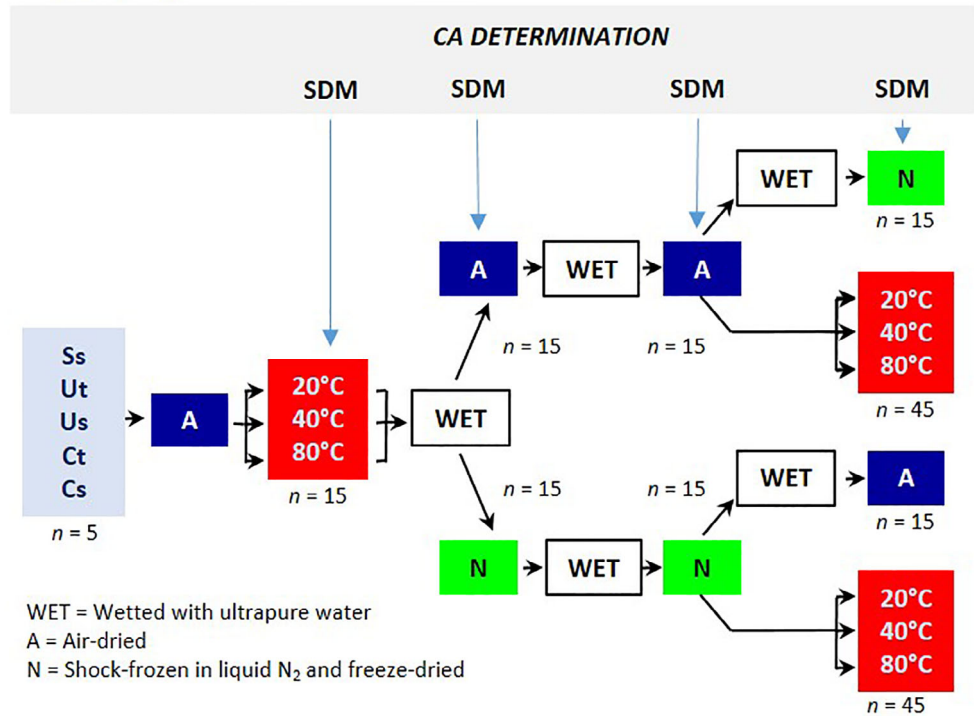
The CA was determined after the first heat treatment, after each wetting-drying cycle, and after the second heat treatment (see Figure 2). To quantify changes in wetting properties caused by heat treatment and wetting-drying cycles, the CA determined after the first 20°C treatment served as a reference because these values were considered to represent the natural wetting properties at an air-dry state. This seems justified as preliminary tests showed that the CA determined after 20°C treatment closely resembled that measured after sampling and air-drying (data not shown). Due to the very limited amount of sample, Sellhorn topsoil (St) material was tested only for the effect of heat treatment at 20°C, 40°C and 80°C and the effect of shock-freezing and freeze-drying of the 80°C-treated material after wetting (80_N).

TABLE 1 Geographic information and basic physical and chemical properties of the soils investigated

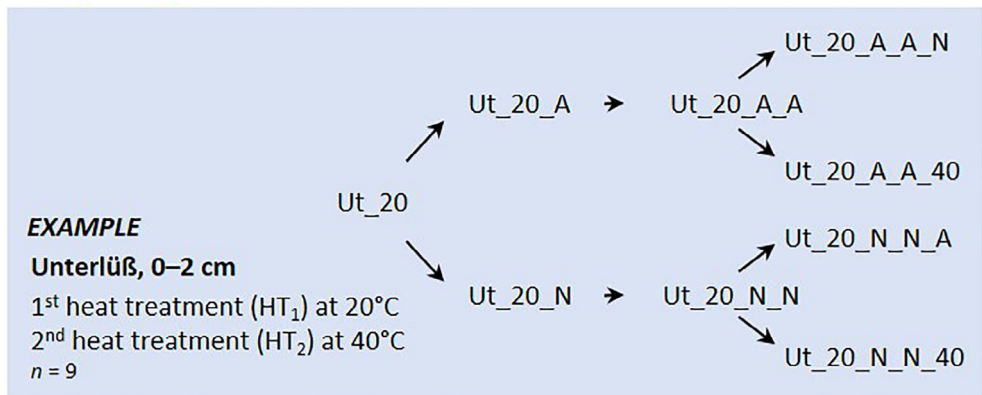
	Sellhorn (S)		Unterlüß (U)		Calvörde (C)	
Coordinates	53°10.359'N, 9°57.151'E		52°49.834'N, 10°18.967'E		52°22.776'N, 11°17.380'E	
Annual precipitation (mm)	816		766		544	
Mean annual temperature (°C)	8.5		8.5		9.1	
Soil use	Forest					
Vegetation	Beech					
Metres above sea level	130		117		75	
Depth (cm)	0–2	4–10	0–2	4–10	0–2	4–10
pH _{CaCl2}	2.97	3.11	2.94	3.05	2.97	3.46
C (g kg ⁻¹)	42.46	16.67	38.34	17.23	63.26	9.72
N (g kg ⁻¹)	2.27	0.91	1.84	0.81	3.22	0.67
C/N	18.7	18.3	20.8	21.3	19.7	14.6
Grain size distribution	(%)					
Sand	84.4	84.4	78.3	78.6	83.9	87.9
Silt	11.3	11.3	17.9	17.9	10.7	8.6
Clay	4.3	4.3	3.9	3.5	5.4	3.5
Texture	Loamy sand		Loamy sand		Loamy sand Sand	

FIGURE 2 Sample preparation scheme (upper graph) and sample key (lower graph). “SDM” (sessile drop method) and arrow indicate contact angle (CA) determination ($n = 6$). The sample key exemplarily is shown for Unterlüß topsoil (Ut), treated at 20°C at the first heat treatment (HT₁) and at 40°C at the second heat treatment (HT₂). S = Sellhorn, U = Unterlüß, C = Calvörde, t = topsoil, s = subsoil

Sample preparation scheme



Sample key scheme



Sample code:
 Xt = Site, topsoil
 Xs = Site, subsoil
 20 = heat treatment at 20°C/24 h
 40 = heat treatment at 40°C/24 h
 80 = heat treatment at 80°C/24 h
 A = Air-dried
 N = Shock-frozen in liquid N₂ and freeze-dried

2.3 | Contact angle measurements

Static sessile drop CAs were measured according to Bachmann et al. (2003) and Goebel, Woche, Abraham, Schaumann, and Bachmann (2013). The CA

quantification was based on images obtained by a CCD-equipped CA microscope (OCA 15, DataPhysics, Filderstadt, Germany; 30 frames per second). Soil material was fixed on a glass slide with double-sided adhesive tape (Bachmann, Horton, van der Ploeg, & Woche, 2000). The

initial CA (designated as CA in the following) was determined when mechanical perturbation stopped after drop placement ($t = 0$ s; ultrapure water, drop volume $1 \mu\text{L}$). The CA was evaluated, after adjustment of a linear baseline, by drop shape analysis (ellipsoidal fit) and fitting tangents on both drop sides with the software SCA20 (DataPhysics; Goebel et al., 2013), giving a CA of each drop as the mean CA of the left and right side of the drop. As an estimate of CA stability, CA was determined again after 5 s (designated as CA_{5s} in the following). The CA is given as the mean of six drops ($n = 6$). In total, 199×6 single CA readings were recorded for the entire sample set.

2.4 | XPS measurements

X-ray photoelectron spectroscopy (XPS) analysis was carried out with an Axis Ultra DLD device (Kratos Analytical, Manchester, UK), using monochromatic AlK_{α} radiation (1,486.6 eV, emission current 20 mA, high voltage 12 kV). For measurement, sample material was fixed on a sample bar with carbon conductive tape (Agar Scientific Elektron Technology UK Ltd, Stansted, UK). Recorded were survey spectra (pass energy 160 eV, dwell time 500 ms) and C 1 s and N 1 s detail scans (pass energy 20 eV, dwell time 300 ms) with each three sweeps per measurement cycle at three different spots per sample ($n = 3$), comprising an area of 0.21 mm^2 each. Survey spectra were quantified with the software Vision 2 (Kratos Analytical, Manchester, UK), giving the chemical composition in atomic-% (at.-%). Speciation was performed with the software CasaXPS (Version 1.5, Casa Software Ltd, Wilslow, UK). The C 1 s peak was fitted with four subpeaks, representing $O=C-O$, $O=C-N$ at 289.3 eV (C1, polar bond); $C=O$, $O-C-O$ at 287.8 eV (C2, polar bond); $C-O$, $C-N$ at 286.4 eV (C3, partly polar bond), and $C-C$, $C-H$ at 284.8 eV (C4, non-polar bond; Gerin et al., 2003). The ratio between (C3/C4) (low binding energy, “L”) and (C1/C2) (high binding energy, “H”), was given as $C_{L/H}$. The N 1 s peak was fitted with two subpeaks, representing organic protonated (at 401.3 eV) and non-protonated (at 399.8 eV) N species (Ahimou et al., 2007). Further, the survey C 1 s peak was fitted with two subpeaks to discriminate between polar (C_p) and non-polar C compounds (C_{np} ; Woche et al., 2017). For further technical details we refer to the Supporting Information for this paper and to Woche et al. (2017). XPS spectra were recorded for 20°C and 80°C -treated material and for 80°C -treated material that was wetted and shock-frozen and freeze-dried (80_N; Table S3, Supporting Information). For Unterlüß topsoil (Ut), additionally the impact of air-drying after 80°C treatment and wetting (80_A) and the impact of reversal of the drying

procedure after two times of wetting and air-drying (80_A_A_N) was tested (Table S3, Supporting Information).

2.5 | Statistical analysis

The statistical significance of differences in CA between treatments was tested by the Kruskal-Wallis test combined with Dunn's post-hoc test using R (version 3.6.1; R Core Team, 2019) and the package ‘FSA’. CA data ($n = 6$) of different soils were found to be not significantly different in their relative response to the applied treatments (Figure S2, Tables S1a,b and S2a,b; Supporting Information) and therefore pooled, yielding a total of $n = 36$ (20°C , 40°C , 80°C and 80_N) and $n = 30$ (A, A_A, N, N_N, A_A_N, N_N_A and second heat treatment) CA measurements for the respective treatments. The relationship between two parameters was evaluated by linear regression and tested for significance (p -value) by one-way univariate ANOVA using SigmaPlot 11.0 (Systat Software, Inc., San Jose, CA, USA).

3 | RESULTS

3.1 | Impact of first heat treatment (HT_1) on contact angle

With the exception of Us, all soils were hydrophobic after the first heat treatment at 20°C (HT_{20}), indicated by $CA \geq 90^\circ$. Heat treatment at 40°C (HT_{40}) had, except for Ut, no measurable impact and CA were similar to those of HT_{20} . In contrast, treatment at 80°C (HT_{80}) increased CA generally to $>100^\circ$ (Figure 3; Table S1a, Supporting Information).

Regarding CA stability (CA_{5s}), 20°C and 40°C -treated materials were repellent after 5 s. The HT_{80} variants all exhibited $CA_{5s} > 90^\circ$, indicating a higher persistency of water repellency compared to 20 and 40°C variants. (Figure 3, lower graph; Table S1b, Supporting Information).

It is also worth mentioning that for Calvörde, the site with the lowest annual precipitation, the largest mean CA and CA_{5s} were found.

3.2 | Impact of wetting–drying cycles after first heat treatment (HT_1) on contact angle

The impact of wetting–drying cycles after HT_1 on CA showed similar tendencies for all soils (Figure S2, Supporting Information) and thus is summarized in Figure 4. Displayed for each variant are CAs of all five soils (individual drops,

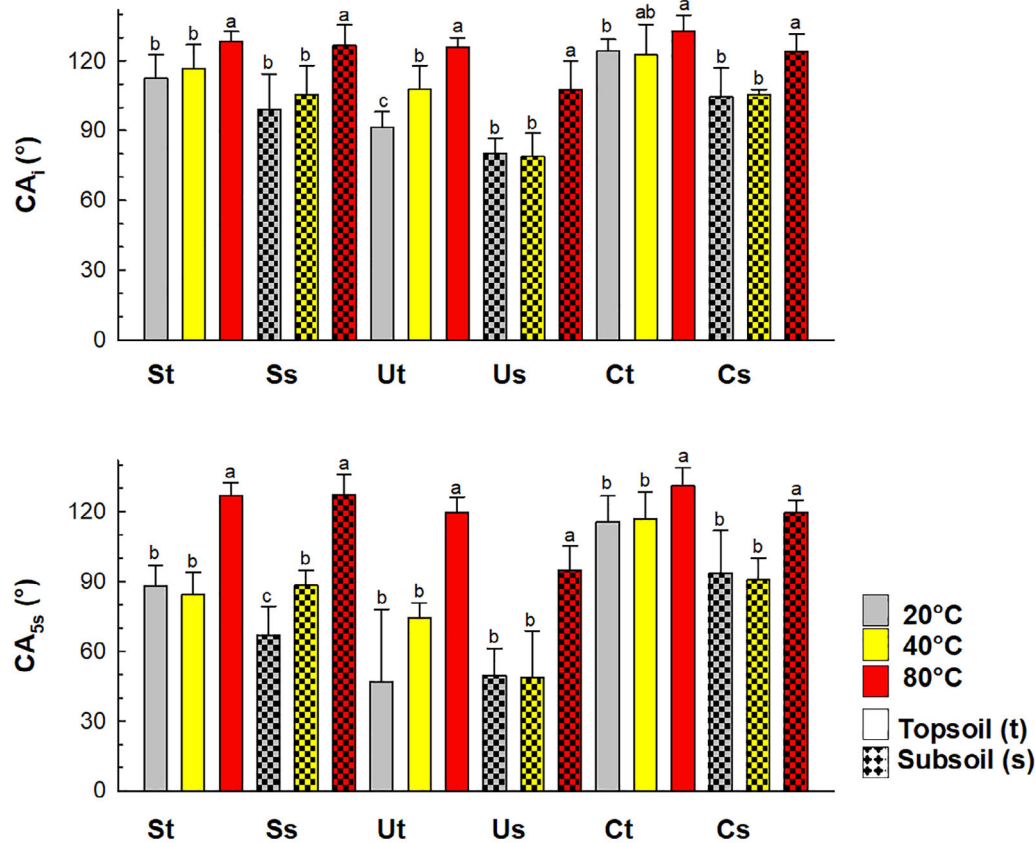


FIGURE 3 Impact of temperature of the first heat treatment (HT₁) on contact angle (CA), measured directly after placement of a drop of water (initial CA, upper graph) and after 5 s (CA_{5s}; lower graph). Bars represent mean values ($n = 6$), with error bars indicating the standard deviation. Different lowercase letters indicate significant differences between the treatments ($p < 0.05$) for each soil. S = Sellhorn, U = Unterlüß, C = Calvörde

$n = 30$) after the first wetting–drying cycle (A: air-drying after wetting; N: shock-freezing and freeze-drying after wetting), after the second wetting–drying cycle (A_A, N_N), and after the third wetting–drying cycle with reversed drying procedure (A_A_N, N_N_A).

As for CAs measured after the first heat treatment (HT₁), CAs were similar for the HT20 and HT40 variants. Air-drying (A, A_A) always led to larger CAs than shock-freezing and freeze-drying (N, N_N). Reversing the mode of the drying procedure increases the CA after two N_N treatments when air-drying follows (N_N_A), and decreases the CA after two A_A treatments when shock-freezing and freeze-drying follows (A_A_N). This scheme was consistent for all heat treatments including the HT80 variant, but for the latter on a higher CA level. Results further show that the original CA measured after HT₁, is not fully re-established after the respective air-drying procedure (A, A_A, N_N_A; Figure 4). This may indicate a period of 4 days of air-drying to be too short to reach an equilibrium state. In line with this, CA stability (CA_{5s}) was reduced after air-drying with comparable values for 20°C and 40°C-treated and markedly greater values for 80°C-treated materials, whereas all shock-frozen and

freeze-dried materials were wettable after 5 s (Figure S2, Table S1b; Supporting Information).

To highlight CA changes, Figure 5 shows relative CA (expressed as percentage) with respect to the CA determined after HT₁. Here, a 100% value indicates no change in relation to the respective CA measured directly after HT₁. The distinct impact of the 80°C treatment is obvious, with values >80% for all air-dried materials (A, A_A, N_N_A). The impact of the preceding drying procedure on CA is clearly visible at reversal of drying procedure with values of <50% for A_A_N and values of >70% for N_N_A materials. The same trends are observed for CA_{5s}, with values of 0% for A_A_N and >40% for N_N_A materials (Figure 5, lower graph).

3.3 | Impact of the second heat treatment (HT₂) on CA after preceding wetting–drying cycles

The impact of HT₂ on CA was also similar for all soils (Figure S2, Supporting Information). Based on the respective CA determined after HT₁, Figure 6 shows the

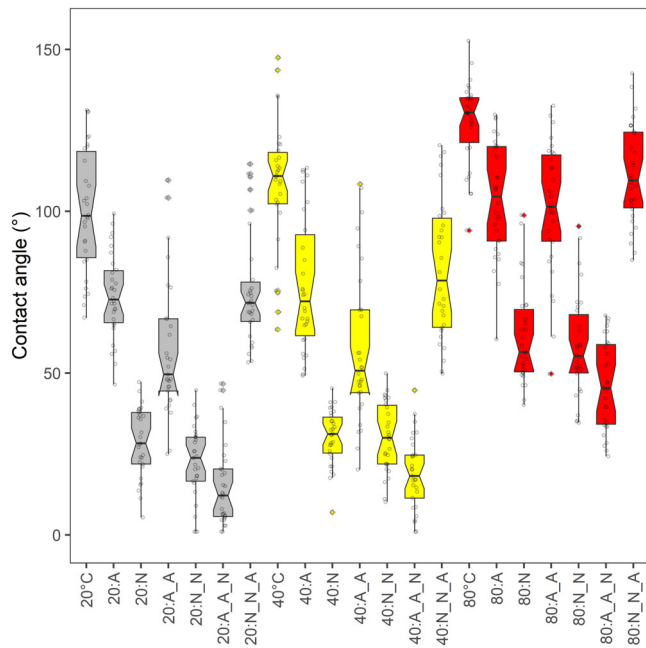


FIGURE 4 Initial contact angle (CA) determined after first heat treatment (HT₁; 20°C, 40°C, 80°C), and after first and second wetting-drying cycle (A, A_A and N, N_N) and reversed drying procedure (A_A_N, N_N_A) for each treatment temperature. Shown are the single values from all materials for the respective treatment ($n = 30$)

relative CA (expressed as percentage) after HT₂ after two times of wetting and either air-drying (A_A) or shock-freezing and freeze-drying (N_N), respectively. In Figure 6, the x axis caption indicates the temperature applied at HT₁, whereas colour indicates the temperature applied at HT₂.

Closer inspection shows that after the two wetting-drying cycles (A_A, N_N) and HT₂, the CA never reached again the original value determined after HT₁ at the same temperature. The next observation is that the 20°C and 40°C variants again behave similarly with respect to the reference CA. When the temperature of HT₂ was 80°C, the CAs always were in the range of those measured after 20°C and 40°C treatment at HT₁. Air-drying (A_A) preceding HT₂ led to larger CAs as compared to N_N preceding HT₂. As CAs of N_N materials were generally only small, the effect of the second treatment at 80°C was more pronounced here. With respect to CA stability (CA_{5s}; Figure 6, lower graphs), observed trends are similar to those of CA_{5s} after HT₁, with an outstanding impact of 80°C treatment.

Generally, after HT₂ the difference in CA observed between air-dried and shock-frozen and freeze-dried materials after two wetting-drying cycles (A_A, N_N; Figure 4) is still observed, although at a lower level.

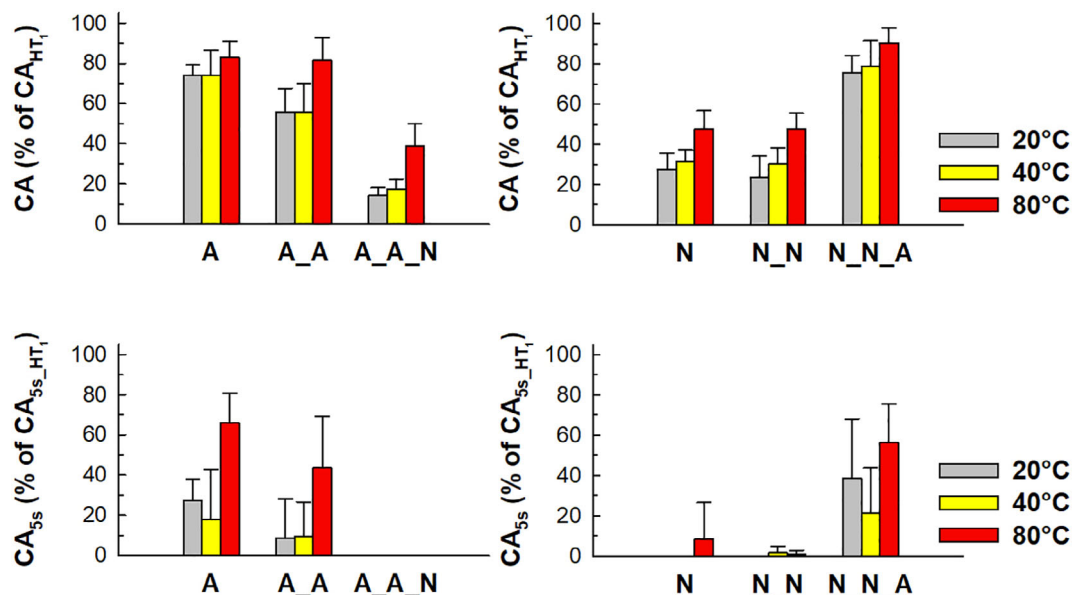


FIGURE 5 Impact of wetting-drying cycles on initial contact angle (CA, upper graphs) and CA after 5 s (CA_{5s}, lower graphs), expressed as percentage of contact angle measured after the first heat treatment (CA_{HT1}). Bars represent mean values ($n = 36$ for 20°C, 40°C and 80_n; otherwise, $n = 30$) for the respective wetting-drying cycle, calculated by pooling results from all sites and depths. Error bars indicate the standard deviation. A value of 100% indicates no difference in contact angle compared to contact angle determined after HT₁

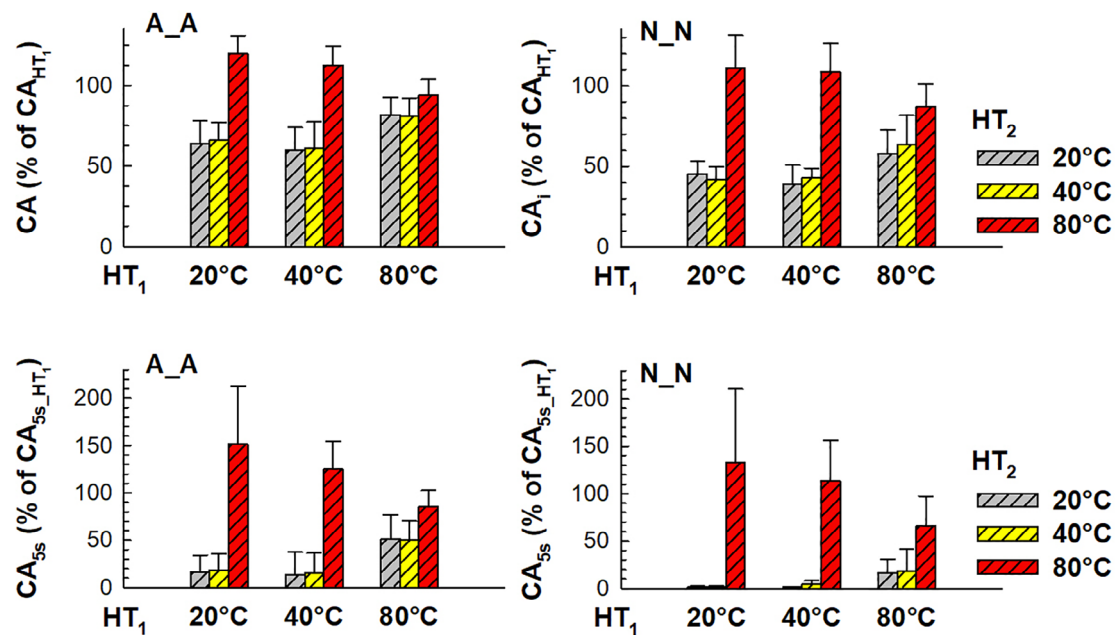


FIGURE 6 Impact of second heat treatment (HT₂) on initial contact angle (CA, upper graphs) and CA after 5 s (CA_{5s}, lower graphs), expressed as percentage of contact angle measured after the first heat treatment (CA_{HT1}). Temperatures given below the columns indicate the temperature of the first heat treatment (HT₁); temperatures given in the legend indicate the temperature applied at the second heat treatment (HT₂), after two wetting–drying cycles (A_A, N_N). Bars represent mean values ($n = 30$), calculated by pooling results from all sites and depths. Error bars indicate the standard deviation. A value of 100% indicates no difference in contact angle compared to contact angle determined after HT₁. Please note the different scaling of the upper and lower graphs

In summary, the initial heat treatment (HT₁) and the subsequent wetting–drying cycles had a consistent impact on wettability of sandy soils from different sites, with a distinct impact of the way dry material is obtained after wetting (Figures 4 and 5). A subsequent second heat treatment (HT₂) at temperatures $\leq 40^\circ\text{C}$ reveals a memory effect regarding the preceding type kind of drying after wetting (A_A, N_N), while HT₂ at temperatures between >40 and 80°C roughly restored the original CA, regardless of the type of drying after wetting preceding HT₂ (Figure 6).

3.4 | X-ray photoelectron spectroscopy (XPS)

3.4.1 | Interface chemical composition

The main elements detected within the outmost interface layer were O and C, followed by Si, N and Al. All subsoils also showed minor amounts of Fe and in some cases traces of Na, Ca and K were found (amount < 0.1 at.-%; Table S3, Supporting Information). The interface chemical composition was similar for Sellhorn and Unterlüß and slightly different for Calvörde, with higher C, N (topsoil) and Al (subsoil) and lower Si contents, especially in

the topsoil. A common feature of all soils was lower C and N and higher O, Si, (Sellhorn and Calvörde) Al and Fe contents in the subsoil (Figure S3, Table S3; Supporting Information).

Treatment at 80°C increased C and decreased O content within the analysis depth, thus decreasing the atomic O/C ratio. With respect to the 20°C treatment, the relative gain in C content was greater than the relative loss in O content within the analysis depth after the 80°C treatment, with a mean ratio between C gain and O loss of around 1.6 ± 0.1 for all materials (Figure S4; Supporting Information). Besides the distinct impact of the 80°C treatment on the O/C ratio (i.e., O and C content), N and Si content was found in tendency to be decreased (Figures S3 and S4; Table S3, Supporting Information).

3.4.2 | C and N speciation

To test the effect of 80°C -treatment and shock-freezing and freeze-drying of wetted material on single C and N compounds, C 1s and N 1s detail scans and the survey C 1s peak were fitted. For C compounds, some change in composition after the 80°C treatment was indicated by distinctly (St/Ss, Ut/Us) or slightly (Ct/Cs) decreased $C_{L/H}$ and increased C_{np}/C_p ratios (Table S5, Figure S5;

Supporting Information). For 80_N, the ratios again were slightly increased ($C_{L/H}$) and decreased (C_{np}/C_p), respectively. For Ut, in agreement with larger CA, the opposite trend was indicated after air-drying (variant Ut_80_A). A decreased CA of Ut_A_A_N, however, was only reflected by C_{np}/C_p (ratio similar to Ut_80_N; Table S5; Supporting Information). Regarding N speciation, a higher amount of protonated organic N species was indicated for soils Ut and Ct compared to all other materials, regardless of variant. However, in contrast to C, neither the 80°C treatment nor wetting–drying cycles resulted in defined changes in N speciation. Treatments did not seem to affect specific N compounds (Table S5, Supporting Information).

4 | DISCUSSION

Our findings of $CA > 90^\circ$ after heat treatment at $T > 40^\circ\text{C}$ are in line with earlier observations (Diehl et al., 2014; Gaj et al., 2019; Goebel et al., 2011). Moreover, this present study can demonstrate that the pronounced effect of HT80 on the wetting properties seems to be independent of the total soil organic carbon (SOC) content. The tested soils had a wide span of SOC contents between 10 and 83 g kg⁻¹ (Table 1). Further, our results suggest that the specific process of drying after wetting strongly affects the CA.

Generally, soil wettability depends on the amount of polar and non-polar C-containing functional groups within the CA interphase (Ferguson & Whitesides, 1992; Woche et al., 2017), originating mainly from SOM. In the case of amphiphilic compounds, the molecular orientation has to be considered as conformational changes that may be enforced by the soil water content, as schematically displayed in Figure 1. In the dry state the non-polar ends point towards the pore space, whereas in the wetted state the polar ends are exposed, as suggested conceptually by Doerr et al. (2000). Hence, depending on moisture conditions, either polar or non-polar functional groups form a solid–liquid or a solid–gas transition zone. Air-drying, as occurs naturally, nearly restores the original wetting properties (Doerr et al., 2000), whereas shock-freezing and freeze-drying generally reduced CA to $<90^\circ$, indicating only subcritical repellency in all cases (Figures 4). From these findings we assume that shock-freezing with subsequent freeze-drying is a technique that potentially allows capture of the interfacial molecular structure of the wetted state. This concept is supported by the good agreement between CAs determined for air-dry material and for shock-frozen and freeze-dried air-dry material, which suggests that the shock-freezing /freeze-drying procedure does not per se

affect wettability of the soil particles (data not shown). Shock-freezing has been used before, for example on soil microaggregates isolated by hydration, in order to observe the spatial arrangement of OM in soil at high resolution (Lehmann et al., 2008), but to our best knowledge our study for the first time indicates that the shock-freezing/freeze-drying procedure enables assessment of the wetted state CA of the solid interface γ_{SL} . In line with this, the approach supports the empirical concept of Doerr et al. (2000) about the orientation of amphiphilic compounds depending on soil water content. The subcritical repellency level of the 80_N materials at the same time indicates the surface free energy of the wetted state to be distinctly increased compared to that of the air-dry state. Thus, in addition to changes in surface free energy due to adsorbed water molecules, an increased amount of polar functional groups pointing towards pore space by reorientation of amphiphilic compounds under wet conditions can be assumed to be responsible for increasing wettability. With respect to applied heat treatment, moreover, the results of our study revealed clearly for the tested sandy topsoil and upper subsoil samples from different sites a significant and for all samples without any exception a consistent, response of wetting properties. Heat treatment at higher temperature (i.e., $>40^\circ\text{C}$) increased water repellency to $CA > 90^\circ$ and reduced the SOM molecular flexibility at the interface. A more rigid structure of SOM by exposure to a temperature above the “glass transition temperature” at approximately 65°C was already suggested through thermal analysis by Schaumann et al. (2005). The upper limit of heat-induced changes in SOM structure will be exposure to temperatures high enough to oxidize SOM, as was shown by Gaj et al. (2019). After treatment at 550°C , interfaces were hydrophilic (i.e., $CA = 0^\circ$) and XPS element analysis indicated clearly bare mineral surfaces. No matter if the samples were treated at 20°C , 40°C or 80°C and either air-dried or shock-frozen and freeze-dried after wetting, CA and XPS analysis confirmed the general relationship between CA and non-polar C-containing functional groups at the interface reported by Woche et al. (2017) with a significant positive linear correlation ($r^2 = 0.42$, $p < = 0.0021$; Figure 7a) that includes the original (20°C treatment) and the treated interfaces (80°C , 80_N, 80_A, 80_A_A_N). Further, from C speciation, non-polar C4 species (C–C, C–H) were found to be significantly positively correlated with CA ($r^2 = 0.22$, $p = 0.0385$; Figure 7b), indicating a relationship between the total amount of non-polar C species and interface wetting properties, as was suggested before (Bachmann et al., 2020).

The observation of decreasing O/C ratio along with increasing CA supports findings of earlier studies (Diehl

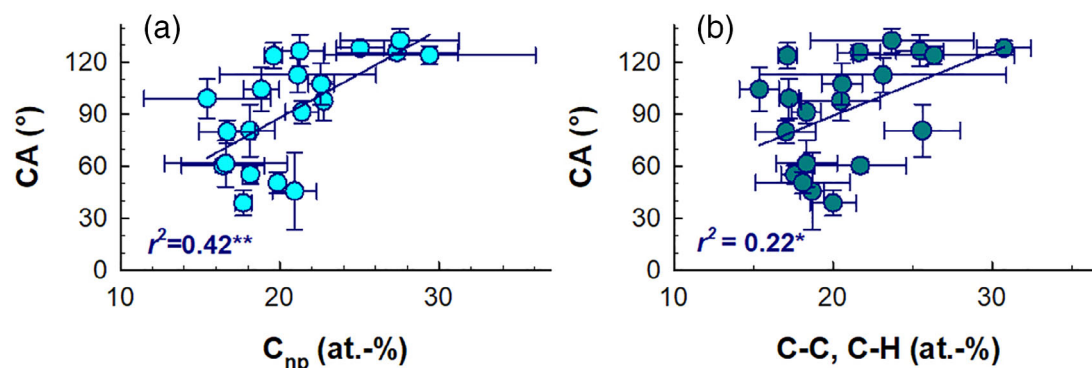


FIGURE 7 Relationship between contact angle (CA) and the amount of (a) non-polar C compounds (C_{np} , in at.-%) and (b) non-polar C-C, C-H species (in at.-%) for all materials tested by X-ray photoelectron spectroscopy (XPS) (Table S3, Supporting Information). Error bars indicate the standard deviation ($n = 6$ for CA data and $n = 3$ for XPS data). The lines represent linear regression fits. Significance level: ** $p < 0.01$; * $p < 0.05$. Data refer to materials after first heat treatment (HT_1)

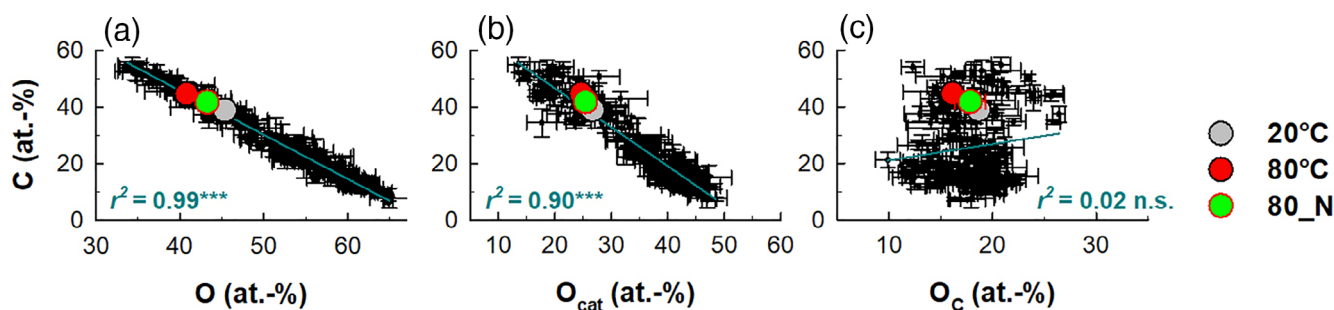


FIGURE 8 Relationship between C content and (a) total O content, (b) the amount of O in bond with mineral-derived cations (O_{cat}), and (c) the amount of O in bond with C (O_C). The lines represent linear regression fits, derived from various datasets, inclusive of the materials of this study ($n = 174$). The pooled data ($n = 18$) of the tested treatments (20°C , 80°C , 80_N) are marked according to the legend. The error bars indicate the standard deviation. Significance level: *** $p < 0.0001$; n.s., not significant. Data refer to materials after first heat treatment (HT_1). The amount of O_{cat} and O_C was calculated after Brodowski et al. (2005)

et al., 2014; Gaj et al., 2019; Woche et al., 2017; Figure S6, Supporting Information). The negative relationship between O/C ratio and CA described earlier (Bachmann et al., 2020; Diehl et al., 2014; Gaj et al., 2019; Gindl, Reiterer, Sinn, & Stanzl-Tschegg, 2004; Krueger et al., 2016; Woche et al., 2017) was, clearly, or at least had a trend of being, supported by a slightly increased O/C ratio at decreased CA for 80_N , (Figure S6, Supporting Information), whereas for material Ut additionally the O/C ratio was indicated to be slightly smaller for Ut_80_A compared to Ut_80_N and Ut_80_A_A_N (Figure S7, Table S4, Supporting Information). The pooled O/C ratio and CA data of the 20°C , 80°C and, 80_N materials fitted well within the general CA vs. O/C ratio relationship published by Woche et al. (2017), with significant differences in CA and O/C ratio between the variants ($p < 0.001$ for CA and $p < 0.001$, 0.002, and 0.030, respectively, for O/C ratio for 20°C vs. 80°C , 20°C vs. 80_N , and 80_N vs. 80°C , respectively; Figure S8,

Supporting Information). In line with this, the generally highly significant negative relationship between O and C content (Woche et al., 2017) was confirmed by the data of this study and by datasets of earlier studies, as summarised in Figure 8a ($n = 174$; $r^2 = 0.99$, $p < 0.0001$). Further, O atoms in bond with mineral-derived cations (O_{cat} , calculated after Brodowski et al., 2005) could be identified to govern this relationship ($r^2 = 0.90$, $p < 0.0001$; Figure 8b), whereas there was no significant relationship between C and O atoms in bond with C atoms (O_C , calculated after Brodowski et al., 2005; $r^2 = 0.02$, $p = 0.084$; Figure 8c).

In contrast to standard bulk analysis, XPS analysis only concerns an interface layer of certain depth of the tested material. As the experiments of the present study were performed in a closed system, that is, no compounds other than water molecules were removed or added, the observed changes in interface chemical composition all are relative and must be ascribed to changes

in chemical composition within the XPS analysis depth. Thus, restructuring of attached SOM with the 80°C treatment can be assumed to be responsible for a decreased signal of the underlying bulk mineral that increases C content relatively. This may be supported by a slight decrease in Si content after the 80°C treatment (Table S3, Figures S3 and S4, Supporting Information) and a significant negative correlation between C and Si content ($r^2 = 0.39$, $p = 0.0032$). Further, the amount of O_{cat} in trend was slightly decreased after 80°C-treatment, also suggesting a higher coverage of the mineral particle surfaces by organic compounds. For the wetted state (variant 80_N), in trend the Si content and amount of O_{cat} were slightly increased compared to the 80°C-treated materials (Table S4, Figure S4, Supporting Information). From the CA observed for the wetted state (variant 80_N), the amount of polar functional groups pointing towards pore spaces is indicated to be increased compared to 80°C and 20°C-treated materials. Again, in conjunction with the observed interface chemical composition, the SOM coating compounds for the 80_N materials seem to be, in tendency restructured again, increasing the amount of bulk mineral within the XPS analysis depth. The considerable standard deviation of the relative changes for pooled O, N, C, Si and O_{cat} data (Figure S4) further may be indicative of locally varying coating thickness and a fractional OM coating, respectively. Because both effects potentially affect the significance of the signals emitted from the mineral surface, a more detailed analysis of the mechanisms regarding the dynamics and geometry of the SOM coatings upon drying and wetting seems not to be reasonable without additional information. In this regard, the close relationship between O and C content (Figure 8a) that is determined by O_{cat} (Figure 8b) may be important. At the same time, it may indicate that the ratio between O and C of the tested materials is not affected by total C content and may explain the similar wetting behaviour of topsoil and subsoil samples with distinctly different bulk C contents (Table 1). In this context, aside from a possibly more fragmented particle coating, the smaller C content observed for the subsoil may indicate a decrease in coating thickness with depth and decreasing C content, as reported also by Bachmann et al. (2020). In contrast to C, in trend N content is decreased after 80°C treatment and in the wetted state (80_N) it is comparable to that after 20°C treatment (Figure S4, Table S3, Supporting Information). This may indicate that N compounds are less involved in SOM structural reorganization and may suggest the presence of less flexible substances such as microorganisms or/and their products (e.g., extracellular polymeric substances [EPS]) on mineral surfaces (Omoike & Chorover, 2004; Zethof et al., 2020).

Knowledge of the CA hysteresis as a basic characterisation of the wetting properties in either the wet or dry state can be considered as the link to identify factors that determine the hysteretic water retention behaviour of unsaturated waterrepellent soil. Hydraulic models that are mechanistically connected to interfacial soil properties are essential to simulate infiltration or water transport in porous media, which are subject to changing levels of SWR. A corresponding model setup can be implemented in terms of continuum mechanics, for example as a single scaling factor, parameterized in the van Genuchten retention model (van Genuchten, 1980) as demonstrated by Arye, Nadav, and Chen (2007), or it can be used to parameterize hydraulic pore scale models including CA information, as published recently by Bernard, Zarebanadkouki, and Carminati (2018) for the temporarily hydrophobic rhizosphere. The relationship between temporal effects of molecular structural reorganization of the interface and the micro-hydraulic response remains at the moment the subject of further research. The increased rigidity of SOM compounds after exposure to temperatures above the glass transition temperature (Schaumann et al., 2005), which may occur during a wildfire, may thus be accompanied by a higher density of hydrophobic SOM compounds at the outermost interface layer, with a potential impact on infiltration capacity or water storage capacity of the soil. A higher frequency of droughts and wildfires due to climate change may thus also affect soil microhydraulic properties, with significant implications for site hydrology on several spatial scales.

5 | CONCLUSIONS

Heat treatment and applied procedures to obtain dry material after wetting had a similar effect on wettability and interface chemical composition of the tested soil materials irrespective of site, depth and SOC content, with the following most significant findings from CA and XPS analysis.

- Treatment at 80°C always rendered the studied soils hydrophobic' (Figures 3 and 4).
- Shock-freezing with subsequent freeze-drying after wetting is indicated to preserve the wetting properties of the wetted state.
- This wetted state only showed subcritical repellency (Figure 4).
- Changes in wetting properties were reflected in changes in interface chemical composition within the XPS analysis depth (Figures 7 and 8; Figures S3 and S4, Supporting Information).

These findings suggest a purely physicochemical effect of heat treatment and wetting on wettability without further impact, for instance, of exudates from roots or microorganisms as typically observed in soil. Thus, we conclude that the observed changes in CA reflect changes in macromolecular SOM structure within the outermost particle interface layer, whose chemical composition determines the wetting properties. From observed CAs, we further conclude that the shock-freezing/freeze-drying procedure applied on wetted soils, as proposed in this study, in our opinion is a new key technique to, at least qualitatively, assess the up to now unknown wettability, as expressed by CA, of the wetted soil particle interfaces. The findings have consequences especially for the hydraulic behaviour of the soils. A mechanistic description of dynamic interfacial properties is key to parameterising dynamic soil water retention curves according to environmental wetting conditions. Further investigations therefore should compare scaling parameters for water retention curves with the respective CA, at best including a time component. In addition, dynamic wettability regarding contact time and the consideration of the energy status of contacting water, that is, the ambient capillary pressure, are further system variables that tentatively need to be considered.

ACKNOWLEDGEMENTS

Financial support provided by the German Research Foundation – DFG (BA 1359/17-1 and CA 921/4-1 for this project is greatly appreciated. We thank the students Lukas Blumenreuter, Ciarán Fitzgerald, Kevin Kaps and Kifah Olba for their excellent support in the laboratory. We further thank two anonymous reviewers for their helpful comments. Open Access funding enabled and organized by Projekt DEAL.

CONFLICT OF INTEREST

The authors declare no potential conflict of interest.


AUTHOR CONTRIBUTIONS

J. B.: conceptualization, methodology, development of the original idea, formal analysis and writing of the original draft. S.K. Woche: writing, review and editing, analysis and interpretation of contact angle data, development of the protocol, and acquisition and analysis of XPS data. M.-O. Goebel: statistical data analysis, writing, review and editing. N. Sepehrnia and S. Söffker: sampling, preparation, investigation and data acquisition. S.K. Woche and M.-O. Goebel: data validation. J. Bachmann: funding acquisition and supervision.

DATA AVAILABILITY STATEMENT

data available on request

ORCID

Joerg Bachmann  <https://orcid.org/0000-0002-8269-3116>
Nasrallah Sepehrnia  <https://orcid.org/0000-0002-9717-9339>

REFERENCES

- Abe, T., & Watanabe, A. (2004). X-ray photoelectron spectroscopy of nitrogen functional groups in soil humic acids. *Soil Science*, *169*, 35–43.
- Adamson, A. W. (1990). *Physical chemistry of surfaces* (5th ed.). New York, NY: John Wiley and Sons.
- Ahimou, F., Boonaert, C. J. P., Adriaensens, Y., Jacques, P., Thonart, P., Paquot, M., & Rouxhet, P. G. (2007). XPS analysis of chemical functions at the surface of *Bacillus subtilis*. *Journal of Colloid and Interface Science*, *309*, 49–55.
- Ahmad, Z., Najeeb, M. A., Shakoor, R. A., Alshraf, A., Al-Muhtaseb, S. A., Soliman, A., & Nazeeruddin, M. K. (2017). Instability in $\text{CH}_3\text{NH}_3\text{PbI}_3$ perovskite solar cells due to elemental migration and chemical composition changes. *Scientific Reports*, *7*, 15406. <https://doi.org/10.1038/s41598-017-15841-4>
- Arye, G., Nadav, I., & Chen, Y. (2007). Short-term reestablishment of soil water repellency after wetting: Effect on capillary pressure-saturation relationship. *Soil Science Society of America Journal*, *71*, 692–702.
- Bachmann, J., Deurer, M., & Arye, G. (2007). Modeling water movement in heterogeneous water-repellent soil: 1. Development of a contact angle-dependent water-retention model. *Vadose Zone Journal*, *6*, 436–445. <https://doi.org/10.2136/vzj2006.0060>
- Bachmann, J., Goebel, M.-O., Krueger, J., Fleige, H., Woche, S. K., Dörner, J., & Horn, R. (2020). Aggregate stability of south Chilean volcanic ash soils – A combined XPS, contact angle, and surface charge analysis. *Geoderma*, *361*, 114022. <https://doi.org/10.1016/j.geoderma.2019.114022>
- Bachmann, J., Goebel, M.-O., & Woche, S. K. (2013). Small-scale contact angle mapping on undisturbed soil surfaces. *Journal of Hydrology and Hydromechanics*, *61*(1), 3–8. <https://doi.org/10.2478/johh-2013-0002>
- Bachmann, J., Horton, R., van der Ploeg, R. R., & Woche, S. (2000). Modified sessile drop method for assessing initial soil–water contact angle of sandy soil. *Soil Science Society of America Journal*, *64*, 564–567.
- Bachmann, J., & McHale, G. (2009). Superhydrophobic surfaces: A model approach to predict contact angle and surface energy of soil particles. *European Journal of Soil Science*, *60*, 420–430.
- Bachmann, J., Woche, S. K., Goebel, M.-O., Kirkham, M. B., & Horton, R. (2003). Extended methodology for determining wetting properties of porous media. *Water Resources Research*, *39* (12), 1353. <https://doi.org/10.1029/2003WR002143>
- Beatty, S. M., & Smith, J. E. (2013). Dynamics of soil water repellency and infiltration in post-wildfire soils. *Geoderma*, *192*, 160–172.
- Benard, P., Zarebanadkouki, M., & Carminati, A. (2018). Impact of pore-scale wettability on rhizosphere rewetting. *Frontiers in Environmental Science*, *6*, 1–8. <https://doi.org/10.3389/fenvs.2018.00016>
- Bos, R., van der Mei, H. C., & Busscher, H. J. (1999). Physico-chemistry of initial microbial adhesive interactions – Its

- mechanisms and methods for study. *FEMS Microbiology Reviews*, 23, 179–230.
- Brodowski, S., Amelung, W., Haumaier, L., Abetz, C., & Zech, W. (2005). Morphological and chemical properties of black carbon in physical soil fractions as revealed by scanning electron microscopy and energy-dispersive X-ray spectroscopy. *Geoderma*, 128, 116–129.
- Buczko, U., Bens, U., & Hüttl, R. F. (2005). Variability of soil water repellency in sandy forest soils with different stand structure under scots pine (*Pinus sylvestris*) and beech (*Fagus sylvatica*). *Geoderma*, 126, 317–336.
- Chassin, P., Jounay, C., & Quiquampoix, H. (1986). Measurement of the surface free energy of calcium-montmorillonite. *Clay Minerals*, 21, 899–907.
- Chibowski, E., Holysz, L., & Szces, A. (2017). Application of thin-layer wicking method for surface free energy determination. *Surface Innovations*, 5, 9–20.
- Clothier, B. E., Vogeler, I., & Magesan, G. N. (2000). The breakdown of water repellency and solute transport through a hydrophobic soil. *Journal of Hydrology*, 231–232, 255–264.
- Dang-Vu, T., Jha, R., Wu, S.-Y., Tannant, D. D., Masliyah, J., & Xu, Z. (2009). Wettability determination of solids isolated from oil sands. *Colloids and Surfaces A*, 337, 80–90.
- DeBano, L. F. (2000). Water repellency in soils: A historical overview. *Journal of Hydrology*, 231–232, 4–32.
- Dekker, L. W., Ritsema, C. J., Oostindie, K., & Boersma, O. H. (1998). Effect of drying temperature on the severity of soil water repellency. *Soil Science*, 163, 780–796.
- Deurer, M., & Bachmann, J. (2007). Modelling water movement in heterogeneous water-repellent soil: 2. A conceptual numerical simulation. *Vadose Zone Journal*, 6, 446–457.
- Diehl, D., Schneckenburger, T., Krueger, J., Goebel, M.-O., Woche, S. K., Schwarz, J., ... Schaumann, G. E. (2014). Effect of multivalent cations, temperature and aging on soil organic matter interfacial properties. *Environmental Chemistry*, 11, 709–718.
- Doerr, S. H., Shakesby, R. A., & Walsh, R. P. D. (2000). Soil water repellency: Its causes, characteristics and hydro-geomorphical significance. *Earth-Science Reviews*, 51, 33–65.
- Drehlich, J. W., Boinovich, L., Chibowski, E., Della Volpe, C., Holysz, L., Marmur, A., & Siboni, S. (2019). Contact angles: History of over 200 years of open questions. *Surface Innovations*, 8, 3–27.
- Dultz, S., Steinke, H., Mikutta, R., Woche, S. K., & Guggenberger, G. (2018). Impact of organic matter types on surface charge and aggregation of goethite. *Colloids and Surfaces A*, 554, 156–168. <https://doi.org/10.1016/J.COLSURFA.2018.06.040>
- Ellerbrock, R. H., Gerke, H. H., Bachmann, J., & Goebel, M.-O. (2005). Composition of organic matter fractions for explaining wettability of three forest soils. *Soil Science Society of America Journal*, 69, 57–66.
- Ellies, A., & Hartge, K. H. (1994). Change of wetting properties of soils as consequence of forest clearing followed by different land use. *Zeitschrift für Kulturtechnik Und Landentwicklung*, 35, 358–364.
- Ferguson, G. S., & Whitesides, G. M. (1992). Thermal reconstruction of the functionalized interface of polyethylene carboxylic acid and its derivatives. In M. E. Schrader & G. Loeb (Eds.), *Modern approaches to wettability – Theory and applications* (pp. 143–177). New York, NY: Plenum Press.
- Flogeac, K., Guillon, E., Aplincourt, M., Marceau, E., Stievano, L., Beaunier, P., & Frapart, Y. M. (2005). Characterization of soil particles by X-ray diffraction (XRD), X-ray photoelectron spectroscopy (XPS), electron paramagnetic resonance (EPR) and transmission electron microscopy (TEM). *Agronomy for Sustainable Development*, 25, 345–353.
- Gaj, M., Lamparter, A., Woche, S. K., Bachmann, J., McDonnell, J. J., & Stange, C. F. (2019). The role of matric potential, solid interfacial chemistry, and wettability on isotopic equilibrium fractionation. *Vadose Zone Journal*, 18, 1–11. <https://doi.org/10.2136/vzj2018.04.0083>
- Gerin, P. A., Genet, M. J., Herbillon, A. J., & Delvaux, B. (2003). Surface analysis of soil material by X-ray photoelectron spectroscopy. *European Journal of Soil Science*, 54, 589–603.
- Gindl, M., Reiterer, A., Sinn, G., & Stanzl-Tschegg, S. E. (2004). Effects of surface ageing on wettability, surface chemistry, and adhesion of wood. *Holz Als Roh- Und Werkstoff*, 62, 273–280.
- Goebel, M.-O., Bachmann, J., Reichstein, M., Janssens, I. A., & Guggenberger, G. (2011). Soil water repellency and its implications for organic matter decomposition – Is there a link to extreme climatic events? *Global Change Biology*, 17, 2640–2656.
- Goebel, M.-O., Woche, S. K., Abraham, P. M., Schaumann, G. E., & Bachmann, J. (2013). Water repellency enhances the deposition of negatively charged hydrophilic colloids in a water-saturated sand matrix. *Colloids and Surfaces A*, 431, 150–160.
- Good, R. J. (1992). Contact angle, wetting, and adhesion: A critical review. *Journal of Adhesion Science and Technology*, 6, 1269–1302.
- Hassan, M., Woche, S. K., & Bachmann, J. (2014). How the root zone modifies soil wettability: Model experiments with alfalfa and wheat. *Journal of Plant Nutrition and Soil Science*, 177, 449–458. <https://doi.org/10.1002/jpln.201300117>
- Jaramillo, D. F., Dekker, L. W., Ritsema, C. J., & Hendrickx, J. M. H. (2000). Occurrence of soil water repellency in arid and humid climates. *Journal of Hydrology*, 231, 105–111.
- Kang, H., Lourenco, S. D. N., & Yan, W. M. (2018). Lattice Boltzmann simulation of droplet dynamics on granular surfaces with variable wettability. *Physical Review E*, 98, 012902. <https://doi.org/10.1103/PhysRevE.98.012902>
- Keizer, J. J., Doerr, S. H., Malvarm, M. C., Prats, S. A., Ferreira, R. S. V., Onate, M. G., ... Ferreira, A. J. D. (2008). Temporal variation in topsoil water repellency in two recently burnt eucalypt stands in north-Central Portugal. *Catena*, 74, 192–204.
- Kleber, M., Sollins, P., & Sutton, R. (2007). A conceptual model of organo–mineral interactions in soils: Self-assembly of organic molecular fragments into zonal structures on mineral surfaces. *Biogeochemistry*, 85, 9–24.
- Kobayashi, M. & Matsui, H. (2003). Surface chemical analysis of water repellent forest soil. EGS - AGU - EUG Joint Assembly, Abstracts from the meeting held in Nice, European Geophysical Society, France, 6–11 April 2003, abstract id. 13491.
- Kögel-Knabner, I., Guggenberger, G., Kleber, M., Kandeler, E., Kalbitz, K., Scheu, S., ... Leinweber, P. (2008). Organo–mineral associations in temperate soils: Integrating biology, mineralogy, and organic matter chemistry. *Journal of Plant Nutrition and Soil Science*, 171, 61–82.
- Krueger, J., Boettcher, J., Schmunk, C., & Bachmann, J. (2016). Soil water repellency and chemical soil properties in a beech forest

- soil spatial variability and interrelations. *Geoderma*, 271, 50–62. <https://doi.org/10.1016/j.geoderma.2016.02.013>
- Krueger, J., Heitkötter, J., Leue, M., Schlüter, S., Vogel, H.-J., Marschner, B., & Bachmann, J. (2018). Coupling of interfacial soil properties and bio-hydrological processes: The flow cell concept. *Ecohydrology*, 11, 1–16. <https://doi.org/10.1002/eco.2024>
- Lamparter, A., Bachmann, J., & Woche, S. K. (2010). Determination of small-scale spatial heterogeneity of water repellency in sandy soils. *Soil Science Society of America Journal*, 74, 2010–2012.
- Lavi, B., Marmur, A., & Bachmann, J. (2008). Porous media characterization by the two-liquid method: Effect of dynamic contact angle and inertia. *Langmuir*, 24, 1918–1923.
- Leighton-Boyce, G., Doerr, S. H., Shakesby, R. A., Walsh, R. P. D., Ferreira, A. J. D., Boulet, A. K., & Coelho, C. O. A. (2005). Temporal dynamics of water repellency and soil moisture in eucalypt plantations, Portugal. *Australian Journal of Soil Research*, 43, 269–280.
- Lehmann, J., Solomon, D., Kinyangi, J., Dathe, L., Wirick, S., & Jacobsen, C. (2008). Spatial complexity of soil organic matter forms at nanometre scales. *Nature Geoscience*, 1, 238–242.
- Lewin, M., Mey-Marom, A., & Frank, R. (2005). Surface free energies of polymer materials, additives and minerals. *Polymers Advanced Technologies*, 16, 429–441. <https://doi.org/10.1002/pat.605>
- Mikutta, R., Schaumann, G. E., Gildemeister, D., Bonneville, S., Kramer, M. G., Chorover, J., ... Guggenberger, G. (2009). Biogeochemistry of mineral–organic associations across a long-term mineralogical soil gradient (0.3–4100 kyr), Hawaiian islands. *Geochimica et Cosmochimica Acta*, 73, 2034–2060.
- Moore, G., & Blackwell, P. S. (2001). Water repellence. In G. A. Moore (Ed.), *Soil guide. A handbook for understanding and managing agricultural soils. Bulletin 4343* (pp. 53–63). Perth, Western Australia: Department of Agriculture and Food.
- Moradi, A. B., Carminati, A., Lamparter, A., Woche, S. K., Bachmann, J., Vetterlein, D., ... Oswald, S. E. (2012). Is the rhizosphere temporarily water repellent? *Vadose Zone Journal*, 11. <https://doi.org/10.2136/vzj2011.0120>
- Omoike, A., & Chorover, J. (2004). Spectroscopic study of extracellular polymeric substances from *Bacillus subtilis*: Aqueous chemistry and adsorption effects. *Biomacromolecules*, 5, 1219–1230.
- Padday, J. F. (1992). Spreading, wetting, and contact angles. *Journal of Adhesion Science Technology*, 6, 1347–1358.
- Core Team, R. (2019). *R: A language and environment for statistical computing*. Vienna, Austria: R Foundation for Statistical Computing. Retrieved from <https://www.R-project.org/>
- Reszkowska, A., Bachmann, J., Lamparter, A., Diamantopoulos, E., & Durner, W. (2014). The effect of temperature-induced soil water repellency on transient capillary pressure–water content relations during capillary rise. *European Journal of Soil Science*, 65, 369–376.
- Saulick, Y., Lourenco, S. D. N., Baudet, B. A., Woche, S. K., & Bachmann, J. (2018). Physical properties controlling water repellency in synthesized granular solids. *European Journal of Soil Science*, 69, 698–709.
- Schaumann, G. E., LeBoef, E. J., DeLapp, R., & Hurraß, J. (2005). Thermomechanical analysis of air-dried whole soil samples. *Thermochimica Acta*, 436, 83–89.
- Scott, D. F. (2000). Soil wettability in forested catchments in South Africa; as measured by different methods and as affected by vegetation cover and soil characteristics. *Journal of Hydrology*, 231–232, 87–104.
- Shchegolikhina, A., Kunhi Mouvenchery, Y., Woche, S. K., Bachmann, J., Schaumann, G. E., & Marschner, B. (2014). Cation treatment and drying-temperature effects on nonylphenol and phenanthrene sorption to a sandy soil. *Journal of Plant Nutrition and Soil Science*, 177, 141–149.
- Siebold, A., Walliser, A., Nardin, M., Oppliger, M., & Schultz, J. (1997). Capillary rise for thermodynamic characterization of solid particle surface. *Journal of Colloid and Interface Science*, 186, 60–70.
- Šolc, R., Tunega, D., Gerzabek, M. H., Woche, S. K., & Bachmann, J. (2015). Wettability of organically coated tridymite surface – Molecular dynamics study. *Pure and Applied Chemistry*, 87, 405–413.
- Sposito, G. (1989). *The chemistry of soils*. New York, NY: Oxford University Press.
- Stevenson, F. J. (1994). *Humus chemistry – Genesis, composition, reactions* (2nd ed.). New York, NY: John Wiley & Sons.
- Täumer, K., Stoffregen, H., & Wessolek, G. (2005). Determination of repellency distribution using soil organic matter and water content. *Geoderma*, 125, 107–115.
- Totsche, K. U., Rennert, T., Gerzabek, M. H., Koegel-Knabner, I., Smalla, K., Spittler, M., & Vogel, H.-J. (2010). Biogeochemical interfaces in soil: The interdisciplinary challenge for soil science. *Journal of Plant Nutrition and Soil Science*, 173, 88–99.
- Tschapek, M. (1984). Criteria for determining the hydrophilicity–hydrophobicity of soils. *Journal of Plant Nutrition and Soil Science*, 147, 137–149.
- van Genuchten, M. T. (1980). A closed-form equation for predicting the hydraulic conductivity of unsaturated soils. *Soil Science Society of America Journal*, 44, 892–898.
- van Oss, C. J., & Giese, R. F. (1995). The hydrophilicity and hydrophobicity of clay minerals. *Clays and Clay Minerals*, 43, 474–477.
- van Oss, C. J., Chaudhury, M. K., & Good, R. J. (1988). Interfacial Lifshitz-van der Waals and polar interactions in macroscopic systems. *Chemical Reviews*, 88, 927–941.
- van Oss, C. J., Giese, R. F., & Constanzo, P. M. (1990). DLVO and non-DLVO interactions in hectorite. *Clays and Clay Minerals*, 38, 151–159.
- Woche, S. K., Goebel, M.-O., Kirkham, M. B., Horton, R., van der Ploeg, R. R., & Bachmann, J. (2005). Contact angle of soils as affected by depth, texture, and land management. *European Journal of Soil Science*, 56, 239–251.
- Woche, S. K., Goebel, M.-O., Mikutta, R., Schurig, C., Kaestner, M., Guggenberger, G., & Bachmann, J. (2017). Soil wettability can be explained by the chemical composition of particle interfaces – An XPS study. *Scientific Reports*, 7. <https://doi.org/10.1038/srep42877>
- Young, T. (1805). An essay on the cohesion of fluids. *Philosophical Transactions of the Royal Society of London*, 95, 65–87.
- Zethof, J. H. T., Bettermann, A., Vogel, C., Babin, D., Cammeraat, E. L. H., Solé-Benet, A., ... Kalbitz, K. (2020). Prokaryotic community composition and extracellular polymeric substances affect soil microaggregation in carbonate containing semiarid grasslands. *Frontiers in Environmental Science*, 8, 51. <https://doi.org/10.3389/fenvs.2020.00051>

Zisman, W. A. (1964). Relation of equilibrium contact angle to liquid and solid construction. In R. F. Gould (Ed.), *Contact angle, wettability and adhesion. Advances in Chemistry, Series 43* (pp. 1–51). Washington, DC: American Chemical Society.

SUPPORTING INFORMATION

Additional supporting information may be found online in the Supporting Information section at the end of this article.

How to cite this article: Bachmann J, Söffker S, Sepehrnia N, Goebel M-O, Woche SK. The effect of temperature and wetting–drying cycles on soil wettability: Dynamic molecular restructuring processes at the solid–water–air interface. *Eur J Soil Sci.* 2021;72:2180–2198. <https://doi.org/10.1111/ejss.13102>